

**High-resolution time-resolved extreme ultraviolet spectroscopy on NSTX<sup>a)</sup>**

J. K. Lepson,<sup>1,b)</sup> P. Beiersdorfer,<sup>2</sup> J. Clementson,<sup>3</sup> M. Bitter,<sup>4</sup> K. W. Hill,<sup>4</sup> R. Kaita,<sup>4</sup>  
C. H. Skinner,<sup>4</sup> A. L. Roquemore,<sup>4</sup> and G. Zimmer<sup>4</sup>

<sup>1</sup>*Space Sciences Laboratory, University of California, Berkeley, California 94720, USA*

<sup>2</sup>*Physics Division, Lawrence Livermore National Laboratory, Livermore, California 94550, USA and  
Department of Chemistry and the Chemical Physics Program, University of Puerto Rico, Río Piedras,  
Puerto Rico 00931, USA*

<sup>3</sup>*Physics Division, Lawrence Livermore National Laboratory, Livermore, California 94550, USA*

<sup>4</sup>*Princeton Plasma Physics Laboratory, Princeton, New Jersey 08543, USA*

(Presented 8 May 2012; received 7 May 2012; accepted 4 June 2012;  
published online 23 July 2012)

We report on upgrades to the flat-field grazing-incidence grating spectrometers X-ray and Extreme Ultraviolet Spectrometer (XEUS) and Long-Wavelength Extreme Ultraviolet Spectrometer (LoWEUS), at the National Spherical Torus Experiment (NSTX) at the Princeton Plasma Physics Laboratory. XEUS employs a variable space grating with an average spacing of 2400 lines/mm and covers the 9–64 Å wavelength band, while LoWEUS has an average spacing of 1200 lines/mm and is positioned to monitor the 90–270 Å wavelength band. Both spectrometers have been upgraded with new cameras that achieve 12.5 ms time resolution. We demonstrate the new time resolution capability by showing the time evolution of iron in the NSTX plasma. © 2012 American Institute of Physics. [<http://dx.doi.org/10.1063/1.4731753>]

**I. INTRODUCTION**

The extreme ultraviolet (EUV) region is rich in emission lines that provide important diagnostic information on plasma conditions. For example, the wavelength region between 10 and 70 Å contains the K-shell emission lines of boron, carbon, nitrogen, oxygen, fluorine, and neon ions, as well as the L-shell emission lines of ions with atomic number  $Z = 16$  (sulfur) through  $Z = 28$  (nickel). This region also contains the M-shell and N-shell emission lines of very high- $Z$  elements, such as tungsten, plus various intrashell emission lines from ions of most elements. The wavelength region between 100 and 270 Å contains the K-shell emission lines of lithium ions, and the M-shell emission lines of nickel and iron, which are particularly important for astrophysics. This region also contains emission lines of molybdenum and copper, which can be important in fusion plasmas.

In magnetic fusion devices, this region is investigated spectroscopically mainly in order to diagnose the plasma impurity content.<sup>1</sup> Time-resolved measurements can also provide information on ion transport and plasma heating. The LoWEUS instrument, for example, was recently used to study tungsten transport in NSTX.<sup>2</sup> These measurements, however, suffered from limited time resolution afforded by the Princeton Instruments PI-SX: 1300/VON camera used at the time. This camera provided a frame rate of  $\sim 90$  ms.<sup>3</sup> Faster rates were possible, but with greatly decreased spatial, and thus spectral, resolution. The upgrades we describe below improve this rate to  $\sim 12.5$  ms.

Tokamaks have historically been excellent laboratory sources for producing atomic data relevant for astrophysical observations and to calibrate spectral diagnostics.<sup>4</sup> However, in the past two decades electron beam ion trap sources have been used more heavily to produce the relevant atomic data to calibrate spectral diagnostics because experimental conditions can be easily tailored to a particular need.<sup>5,6</sup> However, the electron densities in electron beam ion traps<sup>7</sup> reach at most only about  $5 \times 10^{12}$  cm<sup>-3</sup> and is typically closer to  $5 \times 10^{11}$  cm<sup>-3</sup>, so they do not go as high as some of the densities found in solar flares. Tokamaks, by contrast, achieve densities as high as  $5 \times 10^{14}$  cm<sup>-3</sup>. Tokamak observations can, therefore, provide calibrations of spectral electron density diagnostics in regimes unavailable to electron beam ion traps. Fast time resolution is important for such measurements in order to accurately relate spectral information to plasma temperature and density.

We have embarked on a series of laboratory measurements to calibrate spectral density diagnostics used for studying astrophysical sources. For this purpose, we have developed a set of grazing-incidence grating spectrometers, which were first used on the Livermore electron beam ion traps<sup>8,9</sup> and subsequently on NSTX and the Alcator C-Mod tokamak.<sup>10-12</sup> The electron density on NSTX has typically been up to  $5 \times 10^{13}$  cm<sup>-3</sup>, although densities as high as  $10^{14}$  cm<sup>-3</sup> have recently been achieved.

**II. INSTRUMENTS AND TIME-RESOLVED SPECTRA**

The X-ray and Extreme Ultraviolet Spectrometer (XEUS) is a flat-field grating spectrometer, which uses a varied line spacing grating with an average spacing of 2400  $\ell$ /mm, providing a line width (FWHM) of  $\sim 0.1$  Å.

<sup>a)</sup>Contributed paper, published as part of the Proceedings of the 19th Topical Conference on High-Temperature Plasma Diagnostics, Monterey, California, May 2012.

<sup>b)</sup>Electronic mail: lepson@ssl.berkeley.edu.

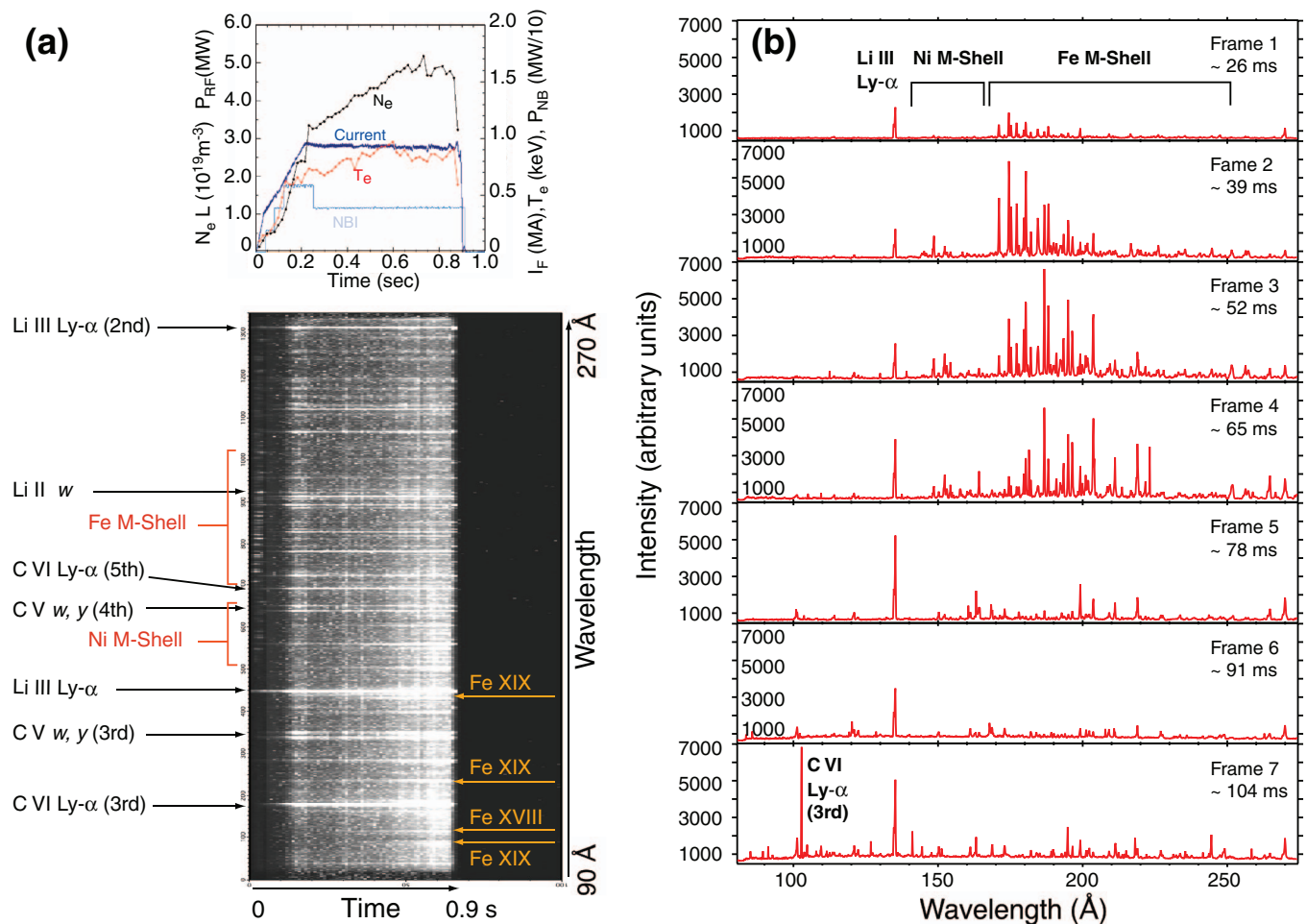


FIG. 1. Time-resolved spectrum of NSTX shot 141 224 taken by LoWEUS. (a) Multi-point Thomson scattering plot and LoWEUS image with prominent lines labeled. (b) Evolution of M-shell nickel and iron during first  $\sim 100$  ms of shot.

The Long-Wavelength Extreme Ultraviolet Spectrometer (LoWEUS) has an average spacing of  $1200 \ell/\text{mm}$ , and a line width (FWHM) of  $\sim 0.3 \text{ \AA}$ .<sup>11</sup>

Both instruments have recently been equipped with a Princeton Instruments PIXIS-XO 100B camera. These detectors consist of a  $1340 \times 100$  pixel back-illuminated charge coupled device (CCD) designed for use with soft x-ray and EUV photons. The small height of the CCD chip and the 2 MHz digitization rate allow for faster readout times than the  $1340 \times 1300$  pixel camera used before, albeit at a reduced spectral intensity. However, in recent years there has been no lack of emission in the EUV from NSTX. In fact, we had to reduce the gain settings to prevent saturation. Hence, faster time resolution did not come at the expense of signal rate. By using on-chip binning of the 100 pixels, which are aligned perpendicular to the spectral dispersion plane, the readout time can be increased even more. Spectra are currently binned to a “depth” of five pixels, which result in a time resolution of 12–13 ms. Further binning can increase the time resolution even more, but multiple images of the same frame are important for determining whether a transient feature is real or due to stray cosmic rays or hard x-rays from the neutral beam injector. We did not observe a decrease in spatial/spectral resolution when using the binning feature with this camera.

A “long” NSTX discharge lasts 1–1.2 s before the shot is disrupted or otherwise ends, but shots often end sooner and are frequently under 1 s in length. In Fig. 1, we show an image of shot 141 224 taken with LoWEUS on 20 Sep 2010. Figure 1(a) shows the multi-point Thomson scattering information of the shot, i.e., electron temperature and electron density. It also shows plasma current and neutral beam power along with the image taken by LoWEUS. Prominent lines in the LoWEUS spectrum are identified, including M-shell iron and nickel and L-shell iron.

The time evolution of individual lines can be clearly seen in Fig. 1. The Lyman- $\alpha$  line of hydrogen-like  $\text{Li}^{2+}$  is the brightest feature across in the spectrum, and the K-shell lines of helium-like  $\text{Li}^{1+}$  are also bright. In addition, the L-shell lines of  $\text{O}^{4+}$  and  $\text{O}^{5+}$ , as well as higher order reflections of the K-shell lines of hydrogen-like  $\text{C}^{5+}$  and helium-like  $\text{C}^{4+}$  are readily seen. M-shell lines of nickel ( $\text{Ni}^{9+} - \text{Ni}^{16+}$ ) and iron ( $\text{Fe}^{7+} - \text{Fe}^{14+}$ ) are seen in the beginning of the shot before the onset of neutral beam injection. The diagonal appearance of these lines graphically illustrates the change in charge balance as the plasma is heated.

The overall emission dramatically increases when the neutral beam sources are turned on after about 100 ms into the discharge, but the M-shell nickel and iron ions “burn out”

and their emission ceases. During neutral beam injection, momentary drops in plasma temperature are readily seen in the image. The temperature and EUV emission level drop almost immediately after the heating is turned off. At this time, L-shell iron (e.g., Fe<sup>17+</sup> – Fe<sup>21+</sup>) often briefly becomes visible just before the end of the shot.

The first seven frames, covering the first 100 ms of the shot are plotted in Fig. 1(b). Lower charge states of M-shell nickel and iron dominate in the earlier frames while higher charge states dominate in the later frames before burning out.

### III. CONCLUSIONS

Upgrades to the time-resolution capabilities of the XEUS and LoWEUS spectrometers at NSTX allow for more detailed studies of the evolution and transport of intrinsic and extrinsic impurities in NSTX plasmas. This capability will be especially valuable for high-Z experiments after the NSTX upgrade (NSTX-U) is completed. Present plans are to begin with molybdenum (TZM), and possibly include tungsten later in the NSTX-U research program.

### ACKNOWLEDGMENTS

This work was performed under the auspices of the U.S. Department of Energy (DOE) under Contract No. DE-AC52-

07NA-27344 by the Lawrence Livermore National Laboratory. Support from the Office of Fusion Energy Sciences Basic and Applied Plasma Science Initiative is gratefully acknowledged.

- <sup>1</sup>B. C. Stratton, M. Bitter, K. W. Hill, D. L. Hillis, and J. T. Hogan, *Fusion Sci. Technol.* **53**, 431 (2008).
- <sup>2</sup>J. Clementson, P. Beiersdorfer, A. L. Roquemore, C. H. Skinner, D. K. Mansfield, K. Hartzfeld, and J. K. Lepson, *Rev. Sci. Instrum.* **81**, 10E326 (2010).
- <sup>3</sup>P. Beiersdorfer, J. K. Lepson, M. Bitter, K. W. Hill, and L. Roquemore, *Rev. Sci. Instrum.* **79**, 10E318 (2008).
- <sup>4</sup>P. Beiersdorfer, M. Bitter, S. von Goeler, and K. W. Hill, *Nucl. Instrum. Methods Phys. Res. B* **43**, 347 (1989).
- <sup>5</sup>P. Beiersdorfer, *Annu. Rev. Astron. Astrophys.* **41**, 343 (2003).
- <sup>6</sup>J. Lepson, P. Beiersdorfer, M. Bitter, and S. M. Kahn, *Can. J. Phys.* **86**, 175 (2008).
- <sup>7</sup>H. Chen, P. Beiersdorfer, L. A. Heeter, D. A. Liedahl, K. L. Naranjo-Rivera, E. Träbert, M. F. Gu, and J. K. Lepson, *Astrophys. J.* **611**, 598 (2004).
- <sup>8</sup>P. Beiersdorfer, J. R. Crespo López-Urrutia, P. Springer, S. B. Utter, and K. L. Wong, *Rev. Sci. Instrum.* **70**, 276 (1999).
- <sup>9</sup>S. B. Utter, G. V. Brown, P. Beiersdorfer, E. J. Clothiaux, and N. K. Podder, *Rev. Sci. Instrum.* **70**, 284 (1999).
- <sup>10</sup>P. Beiersdorfer, M. Bitter, L. Roquemore, J. K. Lepson, and M.-F. Gu, *Rev. Sci. Instrum.* **77**, 10F306 (2006).
- <sup>11</sup>J. Lepson, P. Beiersdorfer, J. Clementson, M. F. Gu, M. Bitter, L. Roquemore, R. Kaita, P. G. Cox, and A. S. Safronova, *J. Phys. B* **43**, 144018 (2010).
- <sup>12</sup>M. L. Reinke, P. Beiersdorfer, N. T. Howard, E. W. Magee, Y. Podpaly, J. E. Rice, and J. L. Terry, *Rev. Sci. Instrum.* **81**, 10D736 (2010).